Citation for published version:
van Houte, S, Ekroth, A, Broniewski, J, Chabas, H, Ashby, B, Bondy-Denomy, J, Gandon, S, Boots, M, Buckling, A & Westra, E 2016, 'The diversity-generating benefits of a prokaryotic adaptive immune system', *Nature*, vol. 532, pp. 385-388. https://doi.org/10.1038/nature17436

DOI:
10.1038/nature17436

Publication date:
2016

Document Version
Peer reviewed version

Link to publication

Publisher Rights
Unspecified

This is the authors' accepted manuscript of an article published in nature and available via:
http://dx.doi.org/10.1038/nature17436

University of Bath

Alternative formats
If you require this document in an alternative format, please contact:
openaccess@bath.ac.uk

General rights
Copyright and moral rights for the publications made accessible in the public portal are retained by the authors and/or other copyright owners and it is a condition of accessing publications that users recognise and abide by the legal requirements associated with these rights.

Take down policy
If you believe that this document breaches copyright please contact us providing details, and we will remove access to the work immediately and investigate your claim.

Download date: 02. Jun. 2023

The diversity-generating benefits of a prokaryotic adaptive immune system

Stineke van Houte[1], Alice K.E. Ekroth[1], Jenny M. Broniewski[1], Hélène Chabas[1,2], Ben Ashby[3,4], Joseph Bondy-Denomy[5], Sylvain Gandon[2], Mike Boots[3,4], Steve Paterson[6], Angus J. Buckling[1] and Edze R. Westra[1]

[1] ESI and CEC, Biosciences, University of Exeter, Cornwall Campus, Penryn, UK.

[2] CEFE UMR 5175, CNRS-Université de Montpellier, Université Paul-Valéry Montpellier, EPHE, 1919, route de Mende 34293 Montpellier Cedex 5, France.

[3] Department of Integrative Biology, University of California, Berkeley, US.

[4] CEC, Biosciences, University of Exeter, Cornwall Campus, Penryn, UK.

[5] Department of Microbiology and Immunology, University of California, San Francisco, 94158, San Francisco, US.

[6] Institute of Integrative Biology, University of Liverpool, UK.

Correspondence and requests for materials should be addressed to E.R.W. (westra.edze@gmail.com), S.v.H. (vanhoute.stineke@gmail.com) or A.B. (A.J.Buckling@exeter.ac.uk).

This is the authors' post-print version. The publisher's version (*Nature* 532, 385-388) is available at dx.doi.org/10.1038/nature17436.

PMID: 27074511

The diversity-generating benefits of a prokaryotic adaptive immune system

Stineke van Houte[1], Alice K.E. Ekroth[1], Jenny M. Broniewski[1], Hélène Chabas[1,2], Ben Ashby[3,4], Joseph Bondy-Denomy[5], Sylvain Gandon[2], Mike Boots[3,4], Steve Paterson[6], Angus J. Buckling[1] and Edze R. Westra[1]

[1] ESI and CEC, Biosciences, University of Exeter, Cornwall Campus, Penryn, UK.

[2] CEFE UMR 5175, CNRS-Université de Montpellier, Université Paul-Valéry Montpellier, EPHE, 1919, route de Mende 34293 Montpellier Cedex 5, France.

[3] Department of Integrative Biology, University of California, Berkeley, US.

[4] CEC, Biosciences, University of Exeter, Cornwall Campus, Penryn, UK.

[5] Department of Microbiology and Immunology, University of California, San Francisco, 94158, San Francisco, US.

[6] Institute of Integrative Biology, University of Liverpool, UK.

Prokaryotic CRISPR-Cas adaptive immune systems insert spacers derived from viruses and other parasitic DNA elements into CRISPR loci to provide sequence-specific immunity[1,2]. This frequently results in high within-population spacer diversity[3-6], but it is unclear if and why this is important. Here, we show that as a result of this spacer diversity, viruses can no longer evolve to overcome CRISPR-Cas by point mutation, which results in rapid virus extinction. This effect arises from synergy between spacer diversity and the high specificity of infection, which greatly increases overall population resistance. We propose that the resulting short-lived nature of CRISPR-dependent bacteria-virus coevolution has provided strong selection for the evolution of sophisticated virus-encoded anti-CRISPR mechanisms[7].

We previously reported that *Pseudomonas aeruginosa* strain UCBPP-PA14 evolves high levels of CRISPR-Cas (Clustered Regularly Interspaced Short Palindromic Repeats; CRISPR-associated) adaptive immunity against virus DMS3vir under laboratory conditions[6]. However, viruses can readily evolve to overcome sequence specific CRISPR immunity[8,9]. To study how CRISPR-Cas impacts virus persistence, we measured titers of virus DMS3vir over time upon infection of either wild type (WT) *P. aeruginosa* or a functional CRISPR-Cas knock-out (CRISPR KO) strain. Virus that infected the WT strain went extinct at 5 days post-infection (dpi) (Fig. 1A), whereas virus infecting the CRISPR KO strain persisted in all replicates until the experiment was terminated at 30 dpi (Fig. 1B). WT bacteria exclusively evolved CRISPR-mediated immunity, while the CRISPR KO strain evolved immunity by mutation, loss or masking of the receptor (i.e. surface mutation) (Extended Data Fig.

47 1A). The observation that CRISPR-Cas drives virus extinct so rapidly was unexpected
48 since viruses can escape CRISPR immunity by a single point mutation[8,9].

49 Virus extinction might result from the high level of spacer diversity that
50 naturally evolves upon virus exposure in this and other CRISPR-Cas systems[3-6]. Both
51 theory and data suggest that host genetic diversity can synergistically reduce the
52 spread of parasites if the infection process is specific (i.e. a parasite genotype can
53 infect a restricted number of host genotypes) and a failed infection results in parasite
54 death[10-18]; assumptions that hold for CRISPR-Cas-virus interactions. While the
55 protective effect of host diversity may be lost following the evolution of single viruses
56 that escape from multiple spacers[10,17], host diversity has the additional benefit of
57 limiting such viral adaptation. Specifically, lower virus population sizes resulting
58 from host diversity[11,12] reduces the probability of escape mutations, and the greater
59 the diversity the more escape mutations needed.

60 To examine these hypotheses, we generated bacterial populations in which we
61 manipulated the level of spacer diversity; we used 48 individual clones with CRISPR-
62 based immunity against virus DMS3vir to generate bacterial populations with five
63 distinct diversity levels: monocultures or polycultures consisting of equal mixtures of
64 either 6, 12, 24 or 48 clones. To allow for direct comparisons, each of the 48 clones
65 was equally represented at each diversity level by adjusting the number of replicate
66 experiments accordingly. Each population was competed against a previously
67 described surface mutant[6] in the presence or absence of virus DMS3vir and virus
68 levels were monitored over time.

69 This experiment revealed a strong inverse relationship between virus
70 persistence and the level of spacer diversity in the bacterial population (Fig. 2). Virus
71 titers remained high in 44 out of 48 replicates when the CRISPR population consisted

72 of a monoculture (Fig. 2A). However, as diversity increased, virus persistence
73 decreased (Fig. 2B-E) and virus was driven extinct rapidly and reproducibly when the
74 CRISPR population consisted of a 48-clone mixture (Fig. 2E).

75 Next, we examined the fitness consequences of generating spacer diversity. In
76 the absence of virus there was no significant effect of diversity on the relative fitness
77 associated with CRISPR-Cas compared to a resistant surface mutant (Extended Data
78 Fig. 1B; $F_{1, 52}$=3.20, p=0.08). However, in the presence of virus CRISPR-associated
79 fitness increased with increasing spacer diversity (Fig. 3; $F_{4,71}$=40.30 p<0.0001 and
80 Extended Data Table 1), with mean fitness increasing 11-fold from monoculture to
81 the highest diversity population. In monoculture, the CRISPR population was
82 outcompeted by the surface mutant (rel. fitness < 1 ; T=-11.68, p<0.0001). However,
83 as diversity increased, the CRISPR population consistently outcompeted the surface
84 mutant (rel. fitness > 1; 6-clones: T=3.05, p=0.0093; 12-clones: T=3.95, p=0.0028;
85 24-clones: T=3.48, p=0.0088; 48-clones: T=3.06, p=0.014; all significant after
86 sequential Bonferroni correction[19]), showing that the generation of spacer diversity is
87 an important fitness determinant of CRISPR-Cas (Fig. 3).

88 Given that all bacterial clones used in the experiment were initially resistant,
89 we hypothesized that the benefit of spacer diversity emerges from an inability of virus
90 to evolve escape mutants. To examine this, virus isolated from each time point (0, 16,
91 24, 40, 48, 64 and 72 hours post-infection) was spotted onto lawns of each of the 48
92 CRISPR clones. As expected, we could not detect escape virus in the ancestral virus
93 (Fig. 4A; left column, indicated in green). However, in 43 of the 48 CRISPR
94 monocultures, virus evolved within 2 days to overcome CRISPR immunity (Fig. 4A;
95 indicated in red). For 5 clones no escape virus could be detected, and virus went
96 extinct in 4 of these instances (Fig. 4A, asterisks). Three of these 5 clones carried

97 multiple spacers targeting the virus, which limits the emergence of escape virus[16]. The
98 emergence of escape virus decreased as diversity increased to 6, 12, 24 and 48
99 CRISPR alleles (Fig. 4); in the latter two, no escape virus could be detected. These
100 phenotypic data were supported by results of deep sequencing of virus genotypes
101 isolated from 1 dpi: there was a significant inverse relationship between host diversity
102 and the accumulation of viral mutations in the target sequences (Extended Data Figs.
103 1CD). This is because virus needs to overcome multiple spacers in the diverse host
104 population if it is to increase in frequency (Extended Data Fig. 1EF). Consistent with
105 a lack of escape virus emerging against all host genotypes, the spacer content of
106 mixed populations of 6, 12, 24 and 48 clones did not increase between t=0 and t=3
107 (Wilcoxon Signed Rank $p>0.2$ for all treatments), whereas monocultures acquired
108 novel spacers in response to emerging escape virus (Wilcoxon Signed Rank W=333,
109 DF=47, $p<0.0001$; Extended Data Fig. 1G). These data show that while escape
110 viruses can clearly evolve against most of the clones, escape viruses do not emerge
111 when these clones are mixed.

112 We hypothesized that the benefit of within-population spacer diversity is
113 because of synergy between the different clones. However, diversity will also increase
114 the chance that the population will contain a single clone with one or more spacers
115 that the virus is unable to overcome. Indeed, we observed 5 clones against which
116 escape mutants were never detected, and presence of these clones in many of the
117 diverse populations could explain the fitness advantage of diversity. To investigate if
118 synergy plays an important role in the benefit of diversity beyond this "jackpot"
119 effect, we compared the fitness of diverse populations with the fitness of the fittest
120 constituent clone, as measured in monoculture. This analysis revealed that synergism
121 contributed an approximately 50% growth rate advantage when in competition with

122 surface mutants (mean ± SEM difference in fitness between mixtures and fittest
123 constituent monoculture = 0.47 ± 0.18; $P < 0.01$).

124 The short-lived nature of coevolution between CRISPR-resistant bacteria and
125 virus escape mutants beyond a host diversity threshold may explain the evolution of
126 sophisticated anti-CRISPR mechanisms to overcome CRISPR-Cas[7]. Indeed, a virus
127 carrying an anti-CRISPR gene[7] was found to persist independent of CRISPR diversity
128 levels (Extended Data Fig. 1HI) and caused similar extinction of CRISPR-resistant
129 monocultures and 48-clone populations that competed against a surface mutant
130 (Fisher's exact test, p=1.0 at t=1, p=0.33 at t=3 dpi; Extended Data Fig. 1J).

131 Finally, to test that our results were not limited to the *P. aeruginosa* PA14
132 Type I-F CRISPR-Cas system, we performed a similar experiment with *Streptococcus*
133 *thermophilus* DGCC7710 clones that evolved resistance against virus 2972 using a
134 Type II-A CRISPR-Cas system. As shown in Extended Data Fig. 2, we found a
135 similar effect of CRISPR resistance allele diversity on virus persistence and escape
136 virus emergence. However, during coevolution experiments the levels of evolved
137 spacer diversity are lower in *S. thermophilus* (data not shown and refs. 4,5), which,
138 consistent with theory[10,17], allows for more persistent coevolution[4,5]. Lower levels of
139 evolved spacer diversity might be due to a more weakly primed CRISPR-Cas
140 system[20-22].

141 Collectively, our data demonstrate that the propensity to generate host genetic
142 diversity is a key fitness determinant of CRISPR-Cas adaptive immune systems
143 because it limits the emergence of escape virus. Consistent with the idea that it is
144 harder for a parasite to adapt to a heterogeneous host population[23], virus rapidly
145 evolved high levels of infectivity on monocultures, but not on a diverse mix of the
146 same host genotypes. Parasites are often invoked as the selective force driving the

evolution of diversity generating mechanisms[23-26]. In most cases, individual-level selection is assumed to be the driver of these traits, because individual benefits are high, and group selective benefits would be opposed by the invasion of individuals who do not pay the fitness costs associated with these mechanisms (e.g. sex and increased mutation rates)[26-28]. In the case of CRISPR-Cas, we speculate that population-level selection may have contributed to its evolution. First, there were large benefits associated with synergy between diverse genotypes. Second, costs of CRISPR-Cas are conditional on virus exposure[6,29] and clones lacking CRISPR immunity cannot invade populations (Extended Data Figs. 3 and 4). Third, the highly structured nature of bacterial populations, and the resulting high relatedness, promotes between-population selection[30]. Future tests of this hypothesis are needed to reconcile the selective forces that have shaped the evolution of CRISPR-Cas systems.

159 **References**

160 1. van der Oost, J., Westra, E. R., Jackson, R. N., Wiedenheft, B. Unravelling the
161 structural and mechanistic basis of CRISPR-Cas systems. *Nature Rev.*
162 *Microbiol.* **12**, 479-92 (2014).
163 2. Barrangou, R., *et al.* CRISPR provides acquired resistance against viruses in
164 prokaryotes. *Science* **315**, 1709-12 (2007).
165 3. Andersson, A.F., Banfield, J. Virus population dynamics and acquired virus
166 resistance in natural microbial communities. *Science* **320**, 1047-50 (2008).
167 4. Paez-Espino, D., *et al*. Strong bias in bacterial CRISPR elements that confer
168 immunity to phage. *Nature Comm.* **4**, 413 (2013).
169 5. Paez-Espino, D. *et al*. CRISPR immunity drives rapid phage genome
170 evolution in *Streptococcus thermophilus*. *MBio* **6**, e00262-15 (2015).
171 6. Westra *et al*. Parasite exposure drives selective evolution of constitutive
172 versus inducible defense. *Curr. Biol.* **25**, 1043-9 (2015).
173 7. Bondy-Denomy, J., Pawluk, A., Maxwell, K. L., Davidson, A. R.
174 Bacteriophage genes that inactivate the CRISPR/Cas bacterial immune
175 system. *Nature* **493**, 429-32 (2013).
176 8. Deveau, H., *et al*. Phage response to CRISPR-encoded resistance in
177 *Streptococcus thermophilus*. *J. Bacteriol.* **190**, 1390-400 (2008).
178 9. Semenova, E. *et al.* Interference by clustered regularly interspaced short
179 palindromic repeats (CRISPR) RNA is governed by a seed sequence. *Proc*
180 *Natl Acad Sci USA*. **108**, 10098-103 (2011).
181 10. Childs, L. M., England, W. E., Young, M. J., Weitz, J. S., Whitaker, R. J.
182 CRISPR-induced distributed immunity in microbial populations. *PLoS One* **9**,
183 e101710 (2014).

184 11. Lively, C. M. The effect of host genetic diversity on disease spread. *Am Nat*
185 **175**, 149-52 (2010).
186 12. King, K. C., Lively, C. M. Does genetic diversity limit disease spread in
187 natural populations? *Heredity* **109**, 199-203 (2012).
188 13. Van Baalen M, Beekman M. The costs and benefits of genetic heterogeneity in
189 resistance against parasites in social insects. *Am Nat* **167**, 568–577 (2006).
190 14. Altermatt F, Ebert D. Genetic diversity of *Daphnia magna* populations
191 enhances resistance to parasites. *Ecol Lett* **11**, 918–928 (2008).
192 15. Schmid-Hempel P, Crozier RH. Polygyny versus polyandry versus parasites.
193 *Phil Trans R Soc Lond B Biol Sci* **354**, 507–515 (1999).
194 16. Levin, B. R., Moineau, S., Bushman, M., Barrangou, R. The population and
195 evolutionary dynamics of phage and bacteria with CRISPR immunity. *PLoS*
196 *Genet.* **9**, e1003312 (2013).
197 17. Iranzo, J., Lobkovsky, A. E., Wolf, Y. I., Koonin, E. V. Evolutionary
198 dynamics of the prokaryotic adaptive immune system CRISPR-Cas in an
199 explicit ecological context. *J. Bacteriol.* **195**, 3834-44 (2013).
200 18. Keesing, F., *et al.* Impacts of biodiversity on the emergence and transmission
201 of infectious diseases. *Nature* **468**, 647-52 (2010).
202 19. Rice, W.R., Analyzing tables of statistical tests. *Evolution* **43**, 223-225 (1989).
203 20. Datsenko, K. A., *et al.* Molecular memory of prior infections activates the
204 CRISPR/Cas adaptive bacterial immunity system. *Nature Comm.* **3**, 945
205 (2012).
206 21. Swarts, D. C., Mosterd, C. van Passel, M. W., Brouns, S. J. CRISPR
207 interference directs strand specific spacer acquisition. *PLoS One*. **7**, e35888
208 (2012).

22. Fineran, P. C., et al. Degenerate target sites mediate rapid primed CRISPR adaptation. *Proc. Natl Acad Sci USA.* **111**, 1629-38 (2014).
23. Hamilton, W. D., Axelrod, R., Tanese, R. Sexual reproduction as an adaptation to resist parasites (a review). *Proc Natl Acad Sci USA* **87**, 3566–3573 (1990).
24. Pal, C., Maciá, M. D., Oliver, A., Schachar, I., Buckling, A. Coevolution with viruses drives the evolution of bacterial mutation rates. *Nature* **450**, 1079-81 (2007).
25. Morran, L. T., Schmidt, O. G., Gelarden, I. A., Parrish R. C. 2nd, Lively, C. M. Running with the red queen: host-parasite coevolution selects for biparental sex. *Science* **333**, 216-8 (2011).
26. Ashby, B., King, K. C. Diversity and the maintenance of sex by parasites. *J. Evol. Biol.* **28**, 511-20 (2015).
27. Lively, C. An epidemiological model of host-parasite coevolution and sex. *J. Evol. Biol.* **23**, 1490-7 (2010).
28. Peters, A.D., Lively, C. The Red Queen and fluctuating epistasis: a population genetic analysis of antagonistic coevolution. *Am. Nat.* **154**, 393-405 (1999).
29. Vale, P.F., et al. Costs of CRISPR-Cas-mediated resistance in *Streptococcus thermophilus*. *Proc. Biol. Sci.* **282**, 20151270 (2015).
30. Gardner, A. & Grafen, A. Capturing the superorganism: a formal theory of group adaptation. *J. Evol. Biol.* **22**, 659-71 (2009).

Acknowledgements

We thank Dan Morley and Suzanne Kay for experimental contributions and Andy Gardner for comments on the manuscript. SVH has received funding from the

European Union's Horizon 2020 research and innovation programme under the Marie Skłodowska-Curie grant agreement No 660039. ERW received funding from the People Programme (Marie Curie Actions) of the European Union's Seventh Framework Programme (FP7/2007-2013) under REA grant agreement No 327606. ERW, AB and MB also acknowledge NERC, BBSRC, the Royal Society, the Leverhulme Trust, the Welcome Trust and the AXA research fund for funding. JBD was supported by the University of California San Francisco Program for Breakthrough in Biomedical Research, the Sandler Foundation, and an NIH Director's Early Independence Award (DP5-OD021344). HC was funded by the Erasmus+ program (European Union), the Explora'Sup program (Région Rhône-Alpes) and the CROUS (French State).

Author contributions

EW, AB and SvH conceived and designed the experiments. HC performed coevolution experiments. SvH, EW, AE and JB performed all competition experiments and associated analysis of virus persistence and host and virus evolution. SP performed and analyzed deep sequencing of virus genomes. JBD supplied virus with anti-CRISPR gene. BA and MB contributed to discussions and provided feedback throughout the project. SG and HC helped to set up the experiments with *Streptococcus thermophilus*. SvH, EW and AB wrote the manuscript.

Author information

Sequence data are available from the European Nucleotide Archive under accession PRJEB12001 and analysis scripts are available from https://github.com/scottishwormboy/vanHoute. Reprints and permissions information

is available at www.nature.com/reprints. The authors declare no conflict of interest. Correspondence and requests for materials should be addressed to: westra.edze@gmail.com, vanhoute.stineke@gmail.com or A.J.Buckling@exeter.ac.uk.

263 **Figure legends**

264 **Figure 1. Evolution of CRISPR-mediated immunity leads to rapid extinction of**
265 **virus.**

266 Titer (pfu/ml) of virus DMS3vir over time upon infection of **A)** WT *P. aeruginosa*
267 and **B)** *P. aeruginosa* strain *csy3::LacZ* (CRISPR KO strain). Each line indicates a
268 biological replicate experiment (n=6). The limit of detection is 200 pfu/ml.

269

270 **Figure 2. Virus persistence inversely correlates with the level of spacer diversity.**

271 Virus titers (pfu/ml) over time upon infection of a bacterial population consisting of
272 an equal mixture of a surface mutant and **A)** a monoculture with CRISPR-mediated
273 immunity (n=48), or polycultures with CRISPR-mediated immunity consisting of **B)**
274 6 clones (n=8), **C)** 12 clones (n=8), **D)** 24 clones (n=6), **E)** 48 clones (n=6). The
275 number of replicates is chosen such that all clones are equally represented in each
276 treatment. Each line indicates a biological replicate experiment; in all cases n is the
277 number of biological replicates. The limit of detection is 200 pfu/ml.

278

279 **Figure 3. The benefit of CRISPR immunity increases with increasing spacer**
280 **diversity.**

281 Relative fitness of bacterial populations with CRISPR-mediated immunity, with
282 spacer diversity as indicated, at 3 days post-infection when competing with a surface
283 mutant. Error bars indicate 95% confidence intervals. In all cases, the number of
284 biological replicates equals the n values given in the legend of Fig. 2.

285

286 **Figure 4. Evolution of virus infectivity is constrained by spacer diversity.**

287 Emergence of virus that overcomes host CRISPR immunity (escape virus) during the
288 experiment shown in Figures 2 (panels A-E correspond to Figure 2 A-E). Table
289 columns correspond to time points where virus was isolated (0, 16, 24, 40, 48, 64 and
290 72 hours post-infection; indicated below the table in days post-infection). Green: no
291 escape virus. Red: escape virus. Bold numbers indicate individual biological
292 replicates, as detailed in the legend of Figure 2. In B-E replicates are separated by
293 bold lines in the table. Numbers between parentheses refer to the clones in the
294 CRISPR population. Asterisks indicate virus extinction.
295
296 **Methods**
297 **Bacterial strains and viruses**
298 *P. aeruginosa* UCBPP-PA14 (WT), *P. aeruginosa* UCBPP-PA14 *csy3::LacZ*
299 (referred to as CRISPR KO, which carries a disruption of an essential *cas* gene and
300 can therefore not evolve CRISPR immunity), the CRISPR KO-derived surface mutant
301 and virus DMS3vir have all been described in ref. 6 and references therein. Phage
302 DMS3vir+*acrF1*, which carries the anti-CRISPR gene *acrF1* (formerly 30-35), was
303 made by inserting *acrF1* into the DMS3vir genome using methods described in ref. 7.
304 *Streptococcus thermophilus* strain DGCC7710 and its virus 2972 have been described
305 in ref. 2.
306
307 **Coevolution experiments**
308 The coevolution experiments shown in Fig. 1 were performed in glass microcosms by
309 inoculating 6 ml M9 supplemented with 0.2% glucose with approximately 10^6 colony
310 forming units (cfu) bacteria from fresh overnight cultures of the WT *P. aeruginosa*
311 UCBPP-PA14 or CRISPR KO strain and adding 10^4 plaque forming units (pfu) of

312 virus DMS3vir, followed by incubation at 37 ºC while shaking at 180 rpm (6
313 replicates). Cultures were transferred daily 1:100 to fresh broth. Virus titers were
314 determined at 0, 3, 5, 11, 17, 22 and 30 days after the start of the coevolution
315 experiment by spotting virus samples isolated by chloroform extraction on a lawn of
316 CRISPR KO bacteria. The analysis of virus immunity was performed by cross-streak
317 assay and PCR as described previously[6].
318
319 **Generation of populations with different levels of CRISPR diversity**
320 For the competition experiments, shown in Figs. 2-4 and Extended Data Figs. 1B-J
321 and Extended Data Figs. 3-4, we generated *P. aeruginosa* populations with varying
322 levels of CRISPR spacer (allele) diversity. To this end, we isolated from the 6
323 replicates of the coevolution experiment (Fig. 1) a total of 48 individual clones that
324 had acquired CRISPR immunity against virus DMS3vir. We have previously shown
325 that individual clones tend to have unique spacers[6]. Using these 48 clones,
326 populations with five different levels of CRISPR spacer (allele) diversity were
327 generated. These populations consisted of: *1)* 1 clone (a monoculture; a clonal
328 population carrying a single spacer); equal mixtures of *2)* 6 clones; *3)* 12 clones; *4)* 24
329 clones and *5)* 48 clones. In total 48 different monocultures (48 x monocultures), 8 x 6-
330 clone populations, 4 x 12-clone populations, 2 x 24-clone populations and 1 x 48-
331 clone population were generated (details of the composition of each population can be
332 found below, under "number of replicate experiments").
333
334 **Competition experiments**
335 Competition experiments were done in glass microcosms in a total volume of 6 ml
336 M9 supplemented with 0.2% glucose. Competition experiments were initiated by

337 inoculating 1:100 from a 1:1 mixture (in M9 salts) of overnight cultures of the
338 appropriate CRISPR population and either the surface mutant (Figs. 2-4 and Extended
339 Data Figs. 1B-J) or the CRISPR KO strain (Extended Data Figs. 3-4). At the start of
340 each experiment 10^9 pfu of virus was added, unless indicated otherwise. Cultures
341 were transferred daily 1:100 into fresh broth. At 0 and 72 hours post-infection (hpi)
342 samples were taken and cells were serially diluted in M9 salts and plated on LB agar
343 supplemented with 50 $\mu g \cdot ml^{-1}$ X-gal (to allow discrimination between WT-derived
344 CRISPR clones (white) and CRISPR KO or surface mutant (blue)). The relative
345 frequencies of the WT strain were used to calculate the relative fitness (rel. fitness =
346 [(fraction strain A at t=x) * (1 – (fraction strain A at t=0))] / [(fraction strain A at t=0)
347 * (1 – (fraction strain A at t=x)]). At 0, 16, 24, 40, 48, 66 and 72 hpi, samples were
348 taken and chloroform extractions were performed to isolate total virus, which was
349 spotted on a lawn of CRISPR KO bacteria for quantification. All subsequent
350 statistical analyses were carried out using JMP (v12) software.
351
352 **Determination of escape virus emergence**
353 To determine the emergence of escape virus during the competition experiments,
354 every isolated virus sample was spotted onto 48 different bacterial lawns,
355 corresponding to each of the different CRISPR clones. This procedure was done for
356 each of the seven time points (see above), to enable us to track the emergence of
357 escape virus against every individual clone over the time course of the experiment.
358
359 **Deep sequencing**
360 Isolated phage samples from t=1 dpi of the competition experiment shown in Fig. 2-4
361 were used to perform deep sequencing of spacer target sites on the phage genomes.

362 To obtain sufficient material, phage were amplified by plaque assay on the CRISPR
363 KO strain. Viruses from all replicates within a single diversity treatment were pooled.
364 As a control, ancestral virus and escape virus from competition between *sm* and
365 monocultures of CRISPR clones 1-3 were processed in parallel. Virus genomic DNA
366 extraction was performed from 5 ml sample at approximately 10^{10} pfu/ml using the
367 Norgen phage DNA isolation kit, following the manufacturer's instructions. Barcoded
368 Illumina Truseq Nano libraries were constructed from each DNA sample with an
369 approximately 350bp insert size and 2x 250bp reads generated on an Illumina MiSeq
370 platform. Reads were trimmed using Cutadapt v1.2.1 and Sickle v1.200 and then
371 overlapping reads merged using Flash v1.2.8 to create high quality sequence at
372 approximately 8000x coverage of DMS3vir per sample. These reads were mapped to
373 PA14 and DMS3vir genomes using bwa mem v0.7.12 and allele frequencies of SNPs
374 within viral target regions quantified using samtools mpileup v0.1.18. Further
375 statistical analyses was performed in R v3.2.2. Sequence data are available from the
376 European Nucleotide Archive under accession PRJEB12001 and analysis scripts are
377 available from https://github.com/scottishwormboy/vanHoute.
378
379 **Determining the acquisition of new spacers**
380 To examine spacer acquisition during the competition experiments shown in Fig. 2-4,
381 we examined by PCR for each diversity treatment the spacer content of 384 randomly
382 isolated clones at both t=0 and t=3 (192 clones per time point). For each replicate
383 experiment, the difference in the total number of spacers between t=0 and t=3 was
384 divided by the number of clones that were examined to calculate the average change
385 in the number of spacers per clone.
386

387 **Number of replicate experiments**

388 To ensure equal representation of each of the 48 clones across the different
389 treatments, the number of replicate experiments for a given diversity treatment was
390 adjusted accordingly, with a total number of replicates of at least 6 for sufficient
391 statistical power. Hence, competition experiments with the 1-clone (monoculture)
392 populations were performed in 48 independent replicates, each corresponding to a
393 unique monoculture of a CRISPR clone (clones 1-48; each clone is equally
394 represented). Competition experiments with the 6-clone populations were performed
395 in eight independent replicates, each corresponding to a unique polyculture population
396 (population 1: equal mixture of clones 1-6; population 2: clones 7-12; population 3:
397 clones 13-18; population 4: clones 19-24; population 5: clones 25-30; population 6:
398 clones 31-36; population 7: clones 37-42; population 8: clones 43-48). Competition
399 experiments with the 12-clone populations were also performed in eight replicates,
400 corresponding to 4 unique polyculture populations (replicate 1 and 2: clones 1-12;
401 replicate 3 and 4: clones 13-24; replicate 5 and 6: clones 25-36; replicate 7 and 8:
402 clones 37-48). Competition experiments with the 24-clone populations were
403 performed in six replicates, corresponding to 2 unique polyculture populations
404 (replicate 1-3: clones 1-24; replicate 4-6: clones 25-48). Competition experiments
405 with the 48-clone populations were performed in six replicates, each corresponding to
406 the same polyculture population (replicate 1-6: clones 1-48).

407

408 **Escape phage degradation and fitness**

409 In the experiment shown in Extended Data Fig. 1EF, approximately 10^8 pfus of either
410 ancestral virus or escape virus, which was isolated from the competitions between
411 monocultures 1-6 and the surface mutant, was used to infect a monoculture of the

412 corresponding CRISPR clone or the 48-clone polyculture. Phage samples were taken
413 at 0, 9, 20 and 28 hpi by chloroform extraction and titrated on a lawn of the CRISPR
414 KO strain. Fitness of each of the escape phages was determined by a competition
415 experiment between ancestral and escape virus; a 50:50 ratio of escape and ancestral
416 phage (10^9 pfus total) was used to infect either a monoculture of the corresponding
417 CRISPR clone or the 48-clone polyculture. Virus samples were taken at t=0 and t=20
418 hpi by chloroform extraction and used in a plaque assay on CRISPR KO. Next,
419 individual plaques (48 plaques per replicate) were isolated and amplified on the
420 CRISPR KO strain. To determine the ratio of escape and ancestral virus, virus from
421 each individual plaque was spotted on a lawn of *1*) CRISPR KO (both ancestral and
422 escape virus form plaques) and *2*) the corresponding CRISPR immune clone (only
423 escape virus can form a plaque).
424
425 **Effect of spacer diversity in *Streptococcus thermophilus***
426 *Streptococcus thermophilus* DGCC7710 was grown in M17 medium supplemented
427 with 0.5% α-lactose (LM17) at 42°C. Virus 2972 was used throughout the
428 experiments. Virus infections were carried out using 10^6 pfus of phage 2972 and
429 10mM $CaCl_2$ to facilitate the infection process. To obtain virus-resistant *S.*
430 *thermophilus* clones, a sample of virus lysate at 24 hpi was plated on LM17 agar
431 plates. Individual colonies were picked and PCR-screened for the acquisition of novel
432 spacers in each of the 4 CRISPR loci, as described in ref. 2. A total of 44 individual
433 clones with a novel spacer in CRISPR1 (see ref. 16 and references therein) were
434 selected to generate 44 monocultures and a single polyculture comprised of a mix of
435 44 clones. These cultures were infected with 10^7 pfu of virus, and samples were taken
436 after the indicated periods of time to isolate virus. We determined virus titers by

437 spotting viral dilutions on lawns of ancestral bacteria, and the emergence of escape
438 virus by spotting virus on lawns corresponding to each of the 44 CRISPR resistant
439 clones.
440
441 **Extended Data Table 1. Tukey HSD of all pairwise comparisons of the data in**
442 **Figure 3.** 1 = monoculture, 6 = 6-clone polyculture, 12 = 12-clone polyculture, 24 =
443 24-clone polyculture, 48 = 48-clone polyculture.
444
445 **Extended Data Figure 1. CRISPR diversity drives virus extinct since virus**
446 **cannot escape by point mutation. A)** Percentage bacteria (WT or CRISPR KO) from
447 the experiment shown in Figure 1 that have evolved CRISPR immunity (white bar),
448 surface immunity (black bar) or remained sensitive (sensitive; grey bars) at 5 days
449 post-infection with virus DMS3vir (n=6 for both treatments). **B)** Relative fitness of
450 CRISPR immune monocultures (single spacer; low diversity, n=48) and polycultures
451 (48 spacers; high diversity, n=6) at 3 days post-infection when competing with a
452 surface mutant (*sm*) in the absence of virus. **C and D)** Deep sequencing analysis of
453 the frequency of mutations seed region and PAM of the target sequence of virus
454 isolated at t=1 from the experiment shown in Fig. 4. **C)** Frequency of point mutation
455 in the target sequence of viral populations isolated from monoculture 1-3 x sm
456 competitions. **D)** Average frequency of point mutation across all target sites in the
457 ancestral virus genome and in the genomes of virus from pooled samples of all
458 biological replicates from a single diversity treatment (monocultures: n=48; 6-clone:
459 n=8; 12-clone: n=8; 24-clone: n=6; 48-clone: n=6). **E and F)** Virus that escapes a
460 single spacer present in a diverse CRISPR population decreases in frequency, despite
461 a fitness benefit over ancestral virus. **E)** Titers (pfu/ml) over time upon infection of
462 monocultures (dotted line) or polycultures of 48 clones (solid line) with

463 approximately 10^8 pfu ancestral (closed circles) or escape (open circles) virus. Escape
464 virus was isolated from monocultures 1-6 x *sm* competitions shown in Fig. 2-4, at 24
465 hpi. N=6 for all experiments. The limit of detection is 200 pfu/ml. **F)** Relative fitness
466 of escape virus at t=1 dpi when competing with ancestral virus on CRISPR resistant
467 monocultures or polycultures consisting of 48 clones. N=6 for both experiments. **G)**
468 For each diversity treatment shown in Figures 2-4 we examined the spacer content of
469 192 randomly isolated clones at both t=0 and t=3 (384 clones in total per diversity
470 treatment). The change in the total number of spacers between t=0 and t=3 was
471 calculated independently for each replicate experiment (number of biological
472 replicates as indicated in legend of Fig. 2) and divided by the number of clones that
473 were examined. The graph indicates the average across the replicates of the change in
474 spacer content per clone. **H, I and J)** Titers (pfu/ml) over time of virus carrying an
475 anti-CRISPR gene (DMS3vir+*acrF1*) following infection of a bacterial population
476 consisting of an equal mixture of a surface mutant and **H)** a monoculture with
477 CRISPR-mediated immunity (n=48) or **I)** a 48-clone polyculture with CRISPR-
478 mediated immunity (n=6). Each clone is equally represented in each treatment. Each
479 line indicates a biological replicate experiment. The limit of detection is 200 pfu/ml.
480 **J)** The number of replicate experiments in which the CRISPR immune population
481 went extinct (no detectable white colonies) at 1 and 3 dpi. In all cases n is the number
482 of biological replicates and error bars indicate 95% CI.
483
484 **Extended Data Figure 2. Virus persistence inversely correlates with the level of**
485 **CRISPR spacer diversity in CRISPR immune populations of *Streptococcus***
486 ***thermophilus*.** Virus titers (pfu/ml) over time upon infection of a bacterial population
487 consisting of **A)** a monoculture with CRISPR-mediated immunity (n=44 biological

488 replicates) or **B)** 44-clone polycultures with CRISPR-mediated immunity (n=28
489 biological replicates). Each clone is equally represented in each treatment. Each line
490 indicates a biological replicate experiment. The limit of detection is 200 pfu/ml. **C)**
491 OD600 of monocultures and polycultures at 1 and 2 days post infection. Error bars
492 indicate 95% confidence intervals. **D)** Emergence of virus mutants that overcome
493 CRISPR-mediated immunity after 0, 16, 24, 40 and 48 hours post-infection. Green
494 indicates no escape virus. Red indicates emergence of escape virus. Escape virus
495 emerged in none of the polyculture experiments.
496
497 **Extended Data Figure 3. Sensitive bacteria are unable to invade bacterial**
498 **populations with CRISPR-mediated immunity in the presence of virus.** Virus
499 titers (pfu/ml) over time upon infection of a bacterial population consisting of an
500 equal mixture of a sensitive CRISPR KO clone and **A)** a monoculture with CRISPR-
501 mediated immunity (n=48), or polycultures with CRISPR-mediated immunity
502 consisting of **B)** 6 clones (n=8), **C)** 12 clones (n=8), **D)** 24 clones (n=6), **E)** 48 clones
503 (n=6). The number of replicates is chosen such that all clones are equally represented
504 in each treatment. Each line indicates a biological replicate experiment. The limit of
505 detection is 200 pfu/ml. **F)** Relative fitness of CRISPR populations at 3 days post-
506 infection during the competitions with the sensitive CRISPR KO described in A-E.
507 Relative fitness of CRISPR populations decreases with increasing spacer diversity due
508 to the rapid virus extinction, which benefits sensitive bacteria, but is higher than 1 in
509 all cases. Error bars indicate 95% CI. **G)** Relative fitness of monoculture (single
510 spacer; low diversity, n=48) and polyculture (48 spacers; high diversity, n=6) at 3
511 days post-infection when competing with the CRISPR KO strain in the absence of
512 virus. Error bars indicate 95% CI. In all cases n is the number of biological replicates.

513

514 **Extended Data Figure 4. Evolution of virus infectivity is constrained by CRISPR**
515 **diversity when CRISPR immune populations compete with sensitive CRISPR**
516 **KO bacteria.** Emergence of virus mutants that overcome CRISPR-mediated
517 immunity during the experiment shown in Extended Data Figure 3. Each column in a
518 table represents a time point (0, 16, 24, 40, 48, 64 and 72 hours post-infection, as
519 indicated below the table (in days post-infection)) where virus was isolated. Green
520 indicates no escape virus. Red indicates emergence of escape virus. Panels A-E
521 correspond to each of the experiments shown in Extended Data Figure 3 A-E. Bold
522 numbers indicate each of the individual biological replicates, as detailed in the legend
523 of Extended Data Fig. 3. In B-E individual replicates are separated by bold lines.
524 Numbers between parentheses indicate the identity of clones that are present in a
525 population with CRISPR-mediated immunity. Asterisks indicate replicate experiments
526 where virus went extinct during the experiment.

527

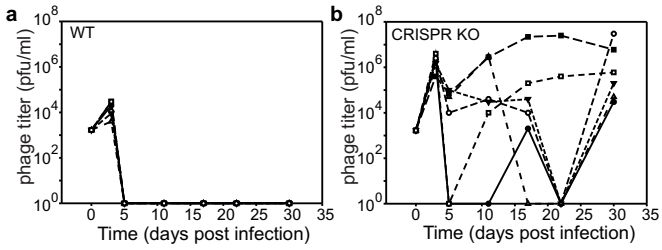
a
WT
phage titer (pfu/ml)
Time (days post infection)
b
CRISPR KO
phage titer (pfu/ml)
Time (days post infection)

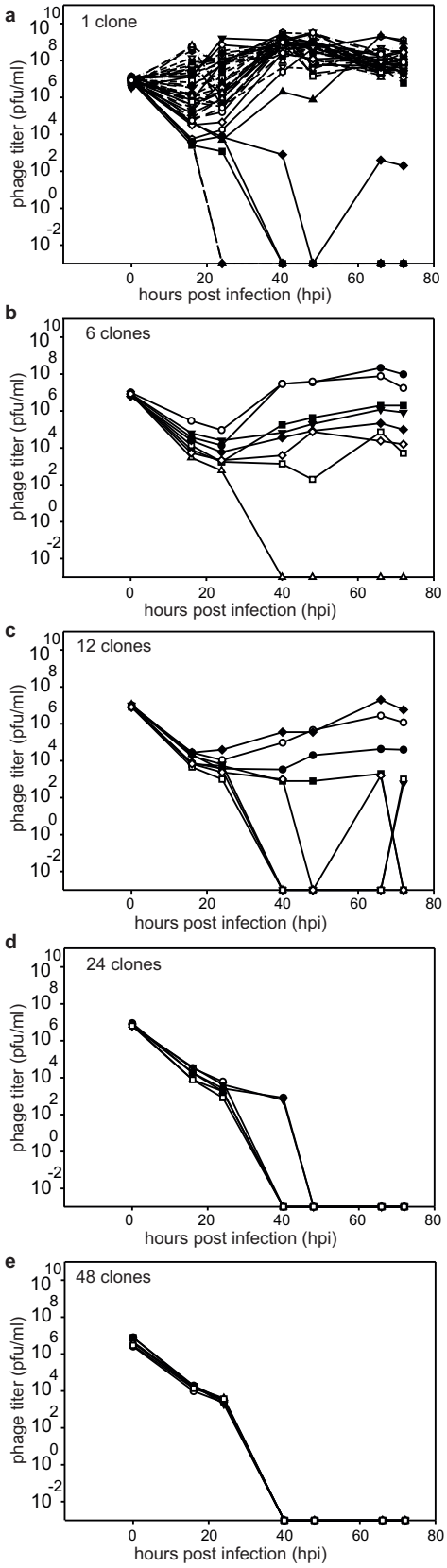
a
1 clone
b
6 clones
c
12 clones
d
24 clones
e
48 clones
phage titer (pfu/ml)
hours post infection (hpi)
0
20
40
60
80

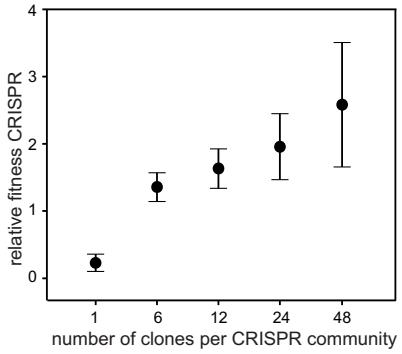
relative fitness CRISPR
4
3
2
1
0
1
6
12
24
48
number of clones per CRISPR community

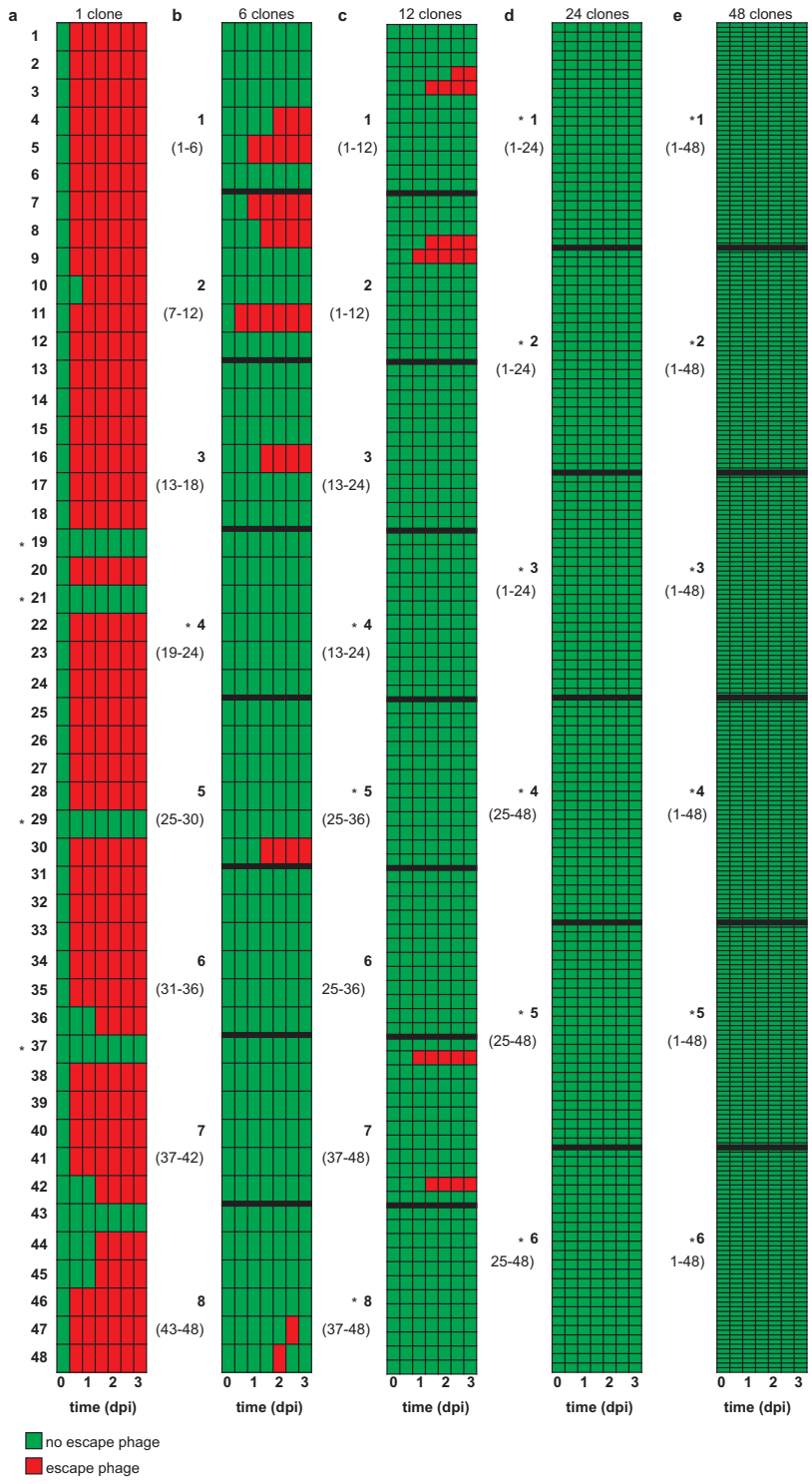
a
1 clone
b
6 clones
c
12 clones
d
24 clones
e
48 clones
time (dpi)
no escape phage
escape phage

531